

'USING MACHINE LEARNING TO PREDICT COLLAPSE OF STEEL STRUCTURES UNDER SEISMIC LOADING

Prakash Gaire¹, Luis Ibarra¹

¹University of Utah, Salt Lake City, USA, luis.ibarra@utah.edu

Abstract: This study applies machine learning (ML) models to predict the collapse limit state of steel moment resisting frame (SMRF) buildings, considering uncertainties in system parameters and input ground motion characteristics. Structural global collapse is affected by a large number of linear and nonlinear system parameters. One of the main goals of the study is to find the effectiveness of ML methods to predict collapse, as the number of system's features is reduced. Because of the lack of sufficient experimental data, an ML approach is followed in which three code-compliant SMRF buildings of varying heights (2, 4 and 8 stories), are evaluated up to the collapse limit state, using nonlinear time history analyses. Variability in system parameters and ground motions, as well as potential correlation among some of the parameters, is considered to generate a database of more than 19,000 realizations of collapsed and non-collapsed systems. The ML models are trained and tested with this database, and the efficiency of the models is categorized using different metrics, such as accuracy, F1-score, precision, and recall.

Six different ML classification-based techniques are employed to predict collapse, finding that boosting algorithms (e.g., AdaBoost and XGBoost) are the best methods for collapse status classification of the evaluated structural systems. Permutation feature importance is applied to identify the main contributors to collapse. The ML models are then retrained using less features, considering first removal of nonlinear deteriorating parameters, and then removal of the hardening nonlinear parameters. The results show that acceleration amplitude, record-to-record variability, and elastic properties of the system are significant predictors of the collapse limit state, as expected; whereas the importance of nonlinear deteriorating parameters depends on the variability of the data source.

Keywords: Machine Learning, SMRFs, Uncertainties, IDA, Collapse

1. Introduction

Uncertainties in structural modeling and seismic hazard influence the structural response assessment and may significantly modify the seismic demands. Detailed nonlinear models and probabilistic methodologies have been carried out to find the significance of these uncertainties in the structural demands (Astroza and Alessandri, 2019; Gokkaya et al., 2016; Ibarra and Krawinkler, 2011; Kazantzi et al., 2014; Liel et al., 2009). The advancements in computer performance capabilities, coupled with the development of advanced algorithms, have significantly increased the utilization of machine learning (ML) in structural and earthquake engineering (Huang and Burton, 2019; Karbassi et al., 2014; Mahmoudi and Chouinard, 2016; Mangalathu and Jeon, 2018a; Mangalathu et al., 2018). These ML techniques have demonstrated their efficacy to design and evaluate the structural demands and limit states of structural components, (Gao and Mosalam,

2018; Kiani et al., 2019; Roeslin et al., 2020; Sun et al., 2021; Zhang et al., 2018). Additionally, ML models allow for easy addition or removal of features, resulting in reliable tools for computing feature importance and uncertainty quantification.

In this study, ML techniques are applied to estimate global collapse employing a comprehensive dataset derived from dynamic analysis of 2-, 4-, and 8-story archetype steel moment resisting frame (SMRF) buildings. The dataset incorporates uncertainties in modeling parameters and a wide array of ground motion data, encompassing 311 different scenarios, and enabling the simulation of a large range of earthquake scenarios. The main goal of the study is to determine the level of information that is required by the different ML algorithms to accurately predict the collapse status of SMRF buildings. For this purpose, a database is generated from dynamic analyses of SMRFs with variation of information about system parameters. Then, several ML algorithms are utilized for three levels of information related to backbone curve of nonlinear springs: i) a baseline feature dataset that includes information about the complete backbone curve with a negative slope for nonlinear beam and column springs, ii) a hardening-only dataset that excludes the parameters defining the backbone softening slope, and iii) an elastic only dataset that just includes features defining the elastic slope of the springs.

2. Methodology

The study is divided into several stages. First, detailed finite element (FE) models of the 2-, 4-, and 8-story SMRF buildings with fixed-based columns were selected as the baseline systems to be evaluated. The buildings and were initially developed by Elkady and Lignos (Elkady, 2016; Elkady and Lignos, 2014) in OpenSees (Mazzoni et al., 2006b). The steel regular buildings have the same plan, elevation, and location. Note that the 2-story building was redesigned to have fixed-base columns, given that initially included pin-based columns. To incorporate uncertainties in modeling parameters, the baseline models were used to generate random realizations based on probabilistic distribution functions of the input parameters. Then, a series of nonlinear time history analyses (THAs) were executed for each realization using incremental dynamic analyses, IDAs (Vamvatsikos and Cornell, 2002) to collect data of maximum inter-story drift ratios up to the collapse limit state (Adam and Ibarra, 2014). Thereafter, ML methods were used to predict building's collapse for the three sets of features.

2.1 Numerical Model

The study is based on three archetype SMRF buildings designed according to USA seismic design provisions (ANSI/AISC 341-10, ANSI/AISC 358-10, ASCE/SEI 7-10). Figure 1 presents the plan and elevation of the archetype buildings, which has two three-bay moment resisting frames in each orthogonal direction. The SMRF was designed for downtown Los Angeles, California (33.996°N, 118.162°W). The design site soil classification was assumed to be class D (i.e., stiff soil). The steel material ASTM A992 Gr. 50 is used.

Two-dimensional (2D) models of the three buildings in the East-West direction were created in OpenSees (McKenna, 1997; Mazzoni et al., 2006), assuming concentrated plasticity. Then, the nonlinear behavior of beams, columns, and panel zones was modeled with elastic beam-column element with end rotational springs. The modified Ibarra-Medina-Krawinkler (IMK) deterioration model was used to model the plastic hinges (Ibarra and Krawinkler, 2005; Lignos and Krawinkler, 2011). Figure 2 shows the monotonic backbone curve for the modified IMK model, defined based on the effective elastic stiffness pre-capping plastic rotation θ_p , post-capping plastic rotation θ_{pc} , effective moment yield strength M_y , maximum or peak moment flexural strength M_c , residual moment strength M_r , and cumulative hysteretic energy dissipation parameter Λ . The central measure of dispersion and standard deviation of the backbone curve parameters was based on the equations proposed by Lignos and Krawinkler (2011), Lignos et al. (2019). A fictitious column was rigidly connected to the SMRF to consider P-Δ effects. On each floor level, the leaning column was subjected to a vertical load equivalent to half of the building's seismic weight minus the cumulative nodal load applied to the MRF columns. The first-floor building's height is 15 ft (4.6m), and the typical floor height is 13 ft (4m). The EW direction MRF bays have a length of 20 ft (6.1 m) and the exterior bays have

a length of 12.2 m, whereas the bays in the NW direction also have a length of 6.1 m. The relatively minor contributions of gravity frames to the lateral stiffness are not considered in the calculations. The THAs considered Rayleigh damping, which was calculated using Equation 1 (Bernal et al., 2015)

$$\xi_s = 1.2 + 4.26 e^{-0.013H} \quad (1)$$

where H is the height of the building in meters.

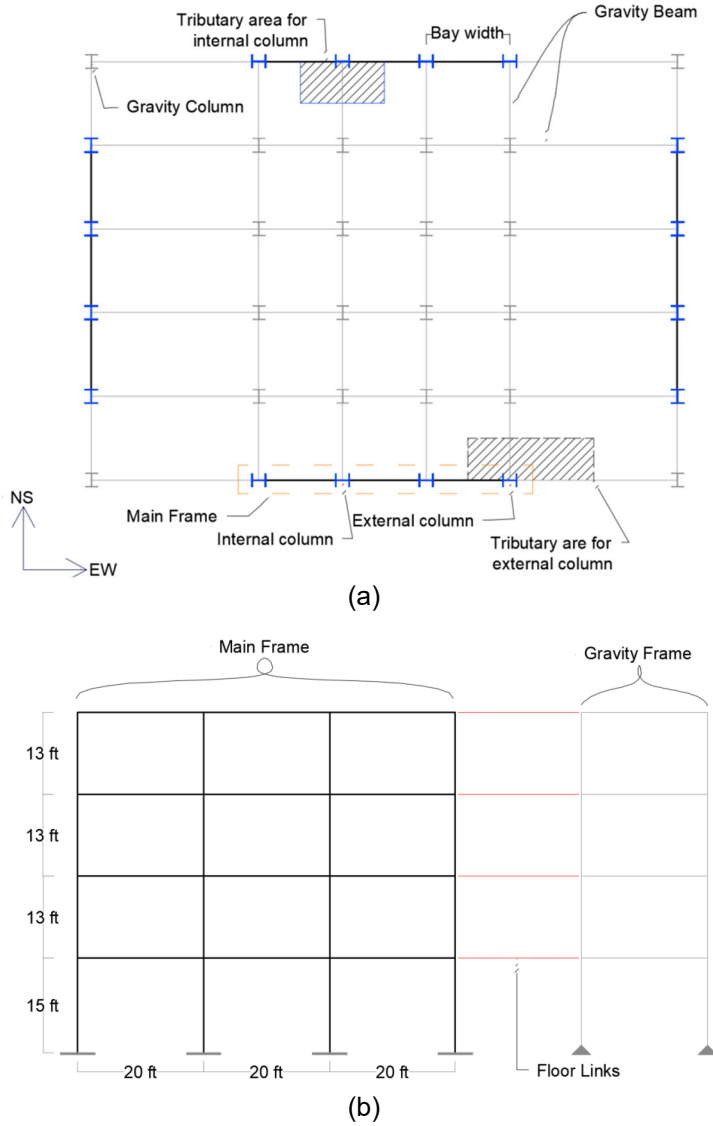


Figure 1: Archetype SMRF building. (a) typical plan view, and (b) elevation of the 4-story building.

3. Generation of database

The collapse/non-collapse database was generated from nonlinear THAs of the above numerical models. The realizations considered uncertainty in the nonlinear spring parameters, which were randomly generated from the probabilistic distribution functions proposed by Lignos and Krawinkler (2011) and Lignos et al. (2019). The springs of beams and columns on each floor were assumed to have the same backbone curve feature values. The rational is that full correlation among elements in the same floor is expected, given that the material batch and construction manpower are likely to be very similar for any particular floor.

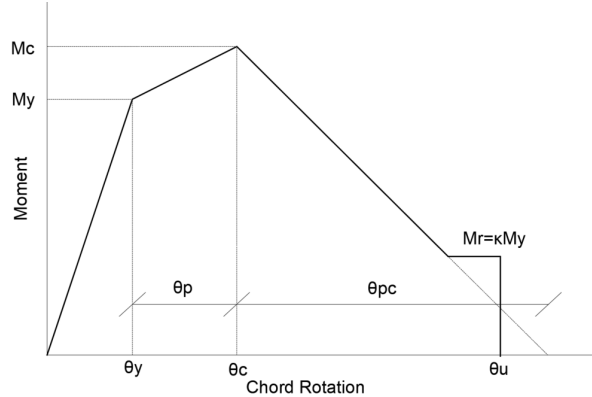


Figure 2: Monotonic backbone curve for the modified IMK model.

Correlation coefficients were introduced to produce partial correlation among the different backbone curve parameters, as it would be expected during design and construction. The backbone parameter partial correlation prevented, for instance, backbone curves with a very large pre-capping plastic rotation θ_p combined with a small post-capping plastic rotation θ_{pc} . Furthermore, a correlation matrix was also implemented to partially correlate the features of the beam and column backbone curves. However, only the features of the springs of the first-floor column and beam were randomly selected. The features of the backbone curve of beam and column springs of upper floors were fully correlated with those of the first floor. Given that the steel shapes changed throughout the building's height, the springs at different floors can still be different, even if they have the same backbone curve features. Full correlation among different floors was implemented to achieve a manageable number of features in the ML algorithms.

A total of 311 seismic records, consisting of 300 far-field (FFGMs) and 11 near-field ground motions (NFGMs) were used in nonlinear THAs. The motions were selected from the PEER ground motion database (Ancheta et al., 2014) and are within the moment magnitude interval from 6.5 to 7.9. The nearest distance to rupture surface (R_{jb}) spans from 0.0 to 43.6 km, and the peak ground acceleration (PGA) falls within the range of 0.10 g to 3.12 g. The FFGMs were taken from 25 different events, with the maximum number of records being around 10% for one particular event, whereas NFGMs were selected from 11 different events. The chosen ground motion set is expected to represent the seismic risk associated with a wide range of building design locations (Ancheta et al., 2014; Eads et al., 2015; FEMA, 2009).

Thereafter, IDAs were carried out for each one of the system parameter realizations, using the same ground motion for each IDA. Collapse was assumed once the stiffness was less than 20% of the initial IDA slope (Vamvatsikos and Cornell, 2002). The slope reduction ("flattening") of the IDA curve serves as an indicator of dynamic instability, where the inter-story drift ratio increases at very high rates, leading to unbounded displacements. In this scenario, one or many stories have a significant displacement, causing the story shear to drop to zero because of P-Δ effect.

A total of 19,190 data points were obtained from the IDA of the three archetype buildings. A data balancing strategy was implemented using the truncation technique, given that an imbalance dataset can lead to biased model training, misleading accuracy, and inefficient models. In the truncation technique, data points from the majority class are randomly selected to match the exact number of data points in the minority class, enhancing the generalization of the dataset because of randomness in selecting majority class. Therefore, a total of 11,266 realizations were obtained for the balanced dataset, which was employed in ML model training and testing.

4. Machine Learning Implementation

Six ML classification algorithms were evaluated, although only six are presented in this document, to predict collapse using different information levels: Logistic Regression, Support Vector Machine (SVM), Decision Tree (DT), Random Forest (RF), Adaptive Boosting (AdaBoost), and eXtreme Gradient Boosting (XGBoost). The training set consisted of 70% of the data, with the 30% remaining data being used for the test set. The efficacy of the ML algorithms was evaluated from confusion matrices in which collapse was considered the “positive event.” The confusion matrix provides results for accuracy, precision, recall, and F1-score, which are metrics based on the number of true positive (TP), true negative (TN), false positive (FP), and false negative (FN) outcomes identified by the ML process.

Accuracy is the ratio of observations correctly predicted to the total number of observations: $\text{Accuracy} = (\text{TP} + \text{TN})/(\text{TP} + \text{TN} + \text{FP} + \text{FN})$. Precision measures how many of the instances predicted as positive by the model are actually positive, and is defined as $\text{Precision} = \text{TP}/(\text{TP} + \text{FP})$. Recall, on the other hand, measures the actual positive instances that are correctly classified by the model: $\text{Recall} = \text{TP}/(\text{TP} + \text{FN})$. In cases where both precision and recall are crucial, the F1-score is utilized, as it represents the harmonic mean of precision and recall: $\text{F1-score} = 2(\text{Precision})(\text{Recall})/(\text{Precision} + \text{Recall})$. The hyperparameters for ML algorithms were tuned along with cross validation with reference to best F1-score. Recall was also monitored because from the perspective of seismic performance assessment, it is crucial not to classify the weaker (collapse class) building as a safe one (non-collapse class).

4.1 Features in ML models

Three different sets of features are employed to develop ML models: i) the baseline feature set including a backbone curve with deteriorating parameters, ii) the hardening models, and iii) the elastic models. Table 1 shows the parameters included in these feature sets. Some building dimension parameters were omitted at this stage of the investigation because the same plan is used for all the buildings, and the story heights are constant. A parameter considering the number of stories was excluded because it is implicitly included through the fundamental period of the structure parameter T_1 . Note that θ_p and θ_{pc} are not included in Table 1, and in its place the hardening (α_s) and post-capping (α_c) stiffness coefficients are used to define the backbone curve nonlinear slopes.

5. Result and discussion

Several regression and classification ML methods were implemented to predict the maximum interstory drift and collapse capacity, respectively. The discussion below focuses on the results of the classification ML methods, which were evaluated via confusion matrix and classification report.

5.1 Confusion matrix:

The confusion matrix for the XGBoost ML method is depicted in Figure 3a for the testing set, given that this ML method provided the best prediction of results for both interstory drifts and collapse capacity. Figure 3a shows that, out of 1690 collapsed buildings, XGBoost correctly predicted 1449, whereas the overall accuracy, precision, recall, and F1-score metrics are coincidentally about 86% due to the quasi-symmetry of this specific confusion matrix. Figure 3b is a combination of the implemented regression and classification XGBoost ML outcomes, and compares the “true” interstory drifts obtained from the numerical models to the predicted drifts from the ML method, which results in a coefficient of determination $R^2 = 0.83$. From the IDA results, the minimum and maximum interstory drift ratios were 0.0015 and 0.1498, respectively. After taking the log on these values and applying a standard scaler, the lower and upper limits moved to -3.26 and 1.78, as shown in Figure 3b. This plot also indicates the correctly predicted collapse and non-collapse outcomes (i.e., TP and TN, respectively), as well as the incorrectly predicted collapsed and non-collapsed cases (i.e., FP and FN, respectively). As expected, the TP and TN predictions are clustered at the two ends of the resulting interstory drifts, whereas the FP and FN results typically occur for intermediate drifts.

Table 1: Parameters included in each feature set.

No.	Feature name	Feature symbol	Baseline models	Hard. models	Elastic models
1	Mass of the building	Mass	✓	✓	✓
2	Fundamental period of the building	T_1	✓	✓	✓
3	Damping ratio	ξ	✓	✓	✓
4	Yield moment for beams	$M_{y,2b}$	✓	✓	✗
5	Yield moment for columns	$M_{y,1c}$	✓	✓	✗
6	Yield rotation for beams	$\theta_{y,2b}$	✓	✓	✗
7	Yield rotation for columns	$\theta_{y,1c}$	✓	✓	✗
8	Strain hardening ratio for beams	$\alpha_{s,2b}$	✓	✓	✗
9	Strain hardening ratio for columns	$\alpha_{s,1c}$	✓	✓	✗
10	Cap to yield strength ratio for beams	$(M_c/M_y)_{2b}$	✓	✗	✗
11	Cap to yield strength ratio for columns	$(M_c/M_y)_{1c}$	✓	✗	✗
12	Cumulative plastic rotation for beams	Λ_{2b}	✓	✗	✗
13	Cumulative plastic rotation for columns	Λ_{1c}	✓	✗	✗
14	Ultimate rotation capacity for columns	$\theta_{u,1c}$	✓	✗	✗
15	Residual strength ratio for columns	$M_{r,1c}$	✓	✗	✗
16	Post-cap stiffness coefficient for beams	$\alpha_{c,2b}$	✓	✗	✗
17	Post-cap stiffness coeff for columns	$\alpha_{c,1c}$	✓	✗	✗
18	Spectral acc. at fundamental period	$S_a(T_1)$	✓	✓	✓
19	Average spectral acceleration to spectral acc. at fundamental period	$S_{a,av}/S_{a,T_1}$	✓	✓	✓
20	Building to predominant GM period	T_1/T_g	✓	✓	✓
21	Ground motion duration	t_{GM}	✓	✓	✓

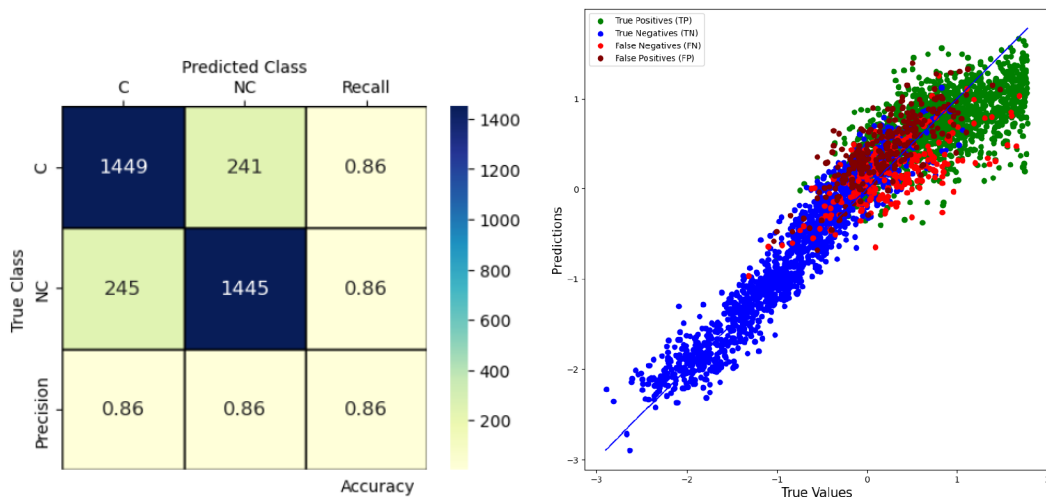


Figure 3. XGBoost ML outcomes. a) Confusion matrix for collapse capacity, and b) predicted vs true maximum interstory drift ratio, including the XGBoost collapse classification.

5.2 Classification report

A summary of classification results for the six ML models and the three feature sets is shown in Figure 4. As can be seen, the performance of ML models collapse prediction for the archetype SMRF appears to be insensitive to features sets with different information levels regarding the properties of nonlinear springs in concentrated plasticity models. This is observed on the different confusion matrix metrics accuracy, F1-score, precision (not shown), and recall, which exhibit minimal variation for the three feature sets.

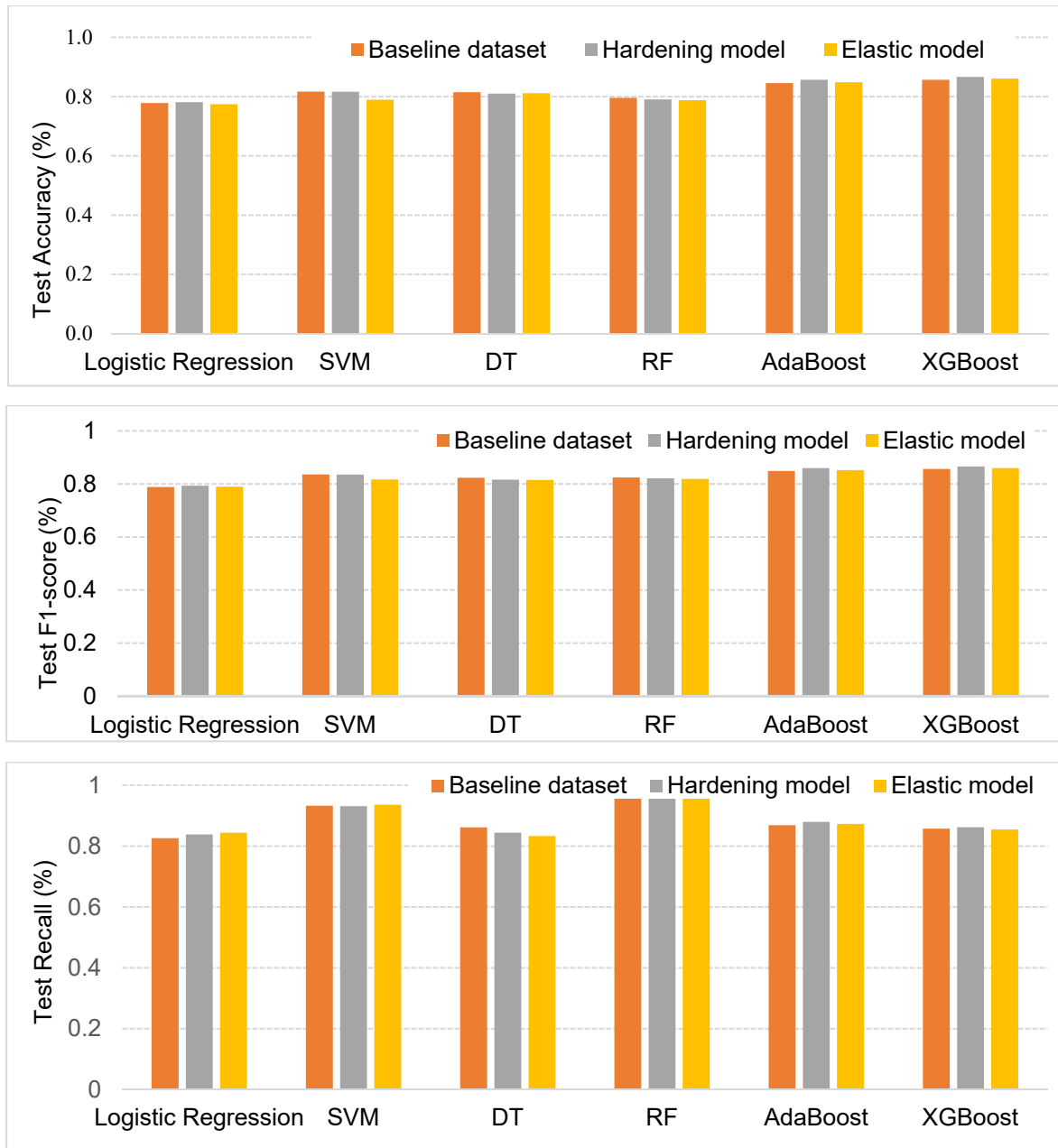


Figure 4: Accuracy, F1-score, and recall for baseline, hardening, and elastic datasets for various ML models.

Interestingly, the hardening and elastic model feature sets did not exhibit a significant reduction on the different estimators, indicating that the backbone nonlinear parameters are not very significant when assessing collapse capacity. This result is not consistent with previous results indicating that the peak strength rotation (θ_c) and the post-capping stiffness ration (α_c) largely contribute to collapse capacity variation (Krawinkler et al., 2010). Collapse assessment is likely not significantly affected by the level of information on the nonlinear backbone parameters because only well-designed conforming buildings were considered in the study. The probabilistic functions of these parameters are size specific and include relatively low dispersion, as observed from the relatively small standard deviation values.

5.3 Permutation feature importance

The permutation feature importance was computed to further investigate the insensitivity of ML models to different levels of information. Permutation feature importance, being model agnostic, is applicable across various ML models. As a best performer, XGBoost classifier is used to get the permutation feature importance (Figure 5).

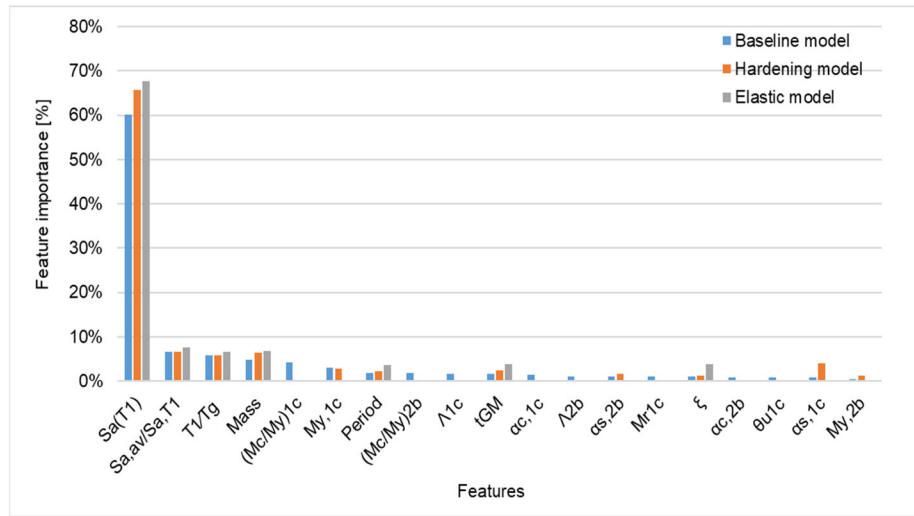


Figure 5. Permutation feature importance for three different levels of information.

As can be seen, $S_a(T_1)$ is the most crucial feature in all three cases of varying information levels, with importance values of 60%, 66%, and 68% for baseline, hardening, and elastic models, respectively. In this exercise, the second and third most important parameters are $S_{a,av}/S_{a,T_1}$ and T_1/T_g , respectively. The former parameter refers to the average spectral acceleration in the interval $(T_1, 2T_1)$ normalized by $S_a(T_1)$. The later parameter normalizes the fundamental period of the system T_1 by the controlling soil period, which was obtained from Fourier analyses. Subsequently, the parameters defining elastic behavior, such as "Mass factor" and period T_1 , rank as the next most significant features. Note that T_1 is largely controlled by the number of stories in the building, but it is also affected by the mass factor, which assigns a variation to the system's mass. These results show that, irrespective of the provided features set, the model's predictions heavily rely on ground motion parameters and features defining the elastic properties of the system. Consequently, omitting features related to nonlinear parameters in the dataset holds minimal significance in ML prediction.

6 CONCLUSIONS

The study examines the ability of several machine learning (ML) methods to estimate global collapse of steel moment resisting frames (SMRFs) under seismic loading, as well as the level of information required to obtain reasonable collapse predictions. Three feature datasets were utilized with varying degrees of information regarding the nonlinear properties of springs in the concentrated plasticity models of code

conforming SMRF archetype buildings. The primary objective was to assess the impact of this information variability on the predictive capabilities of ML models. Six different ML classification models were employed to explore the influence of different information levels. The results were analyzed using classification reports, leading to the following conclusions:

- i. The XGBoost ML method was the best predictor of the collapse of archetype SMRF buildings based on the classification report.
- ii. ML models for predicting collapse exhibit insensitivity to the nonlinear spring parameters of code conforming SMRF buildings.
- iii. The most important parameter for predicting the collapse limit state is identified as $S_a(T_1)$. For modern code conforming buildings, nonlinear parameters related to the backbone curve have little significance in collapse prediction using ML models.

The presented results are considered valid for the type of configurations and seismic demands included in the study.

Acknowledgements

This material is based upon work supported by the National Science Foundation under Award No. 2121169. Any opinions, findings, conclusions or recommendations expressed in this publication are those of the authors and do not necessarily reflect the views of any of the supporting agencies. The authors are also grateful to Dr. Stephen Brown from Aprovechar Lab L3C for his valuable feedback on the implementation of ML methodologies.

References

Adam C., L. Ibarra (2014) "Seismic Collapse Assessment." *Seismic Risk Assessment*. Editors F. and C. Galasso. *Encyclopedia of Earthquake Engineering* – Ed. Springer.

Ancheta T.D., Darragh R.B., Stewart J.P., Seyhan E., Silva W.J., et al. (2014). NGA-West2 database. *Earthquake Spectra*. 30(3):989–1005.

Astroza R., Alessandri A. (2019). Effects of model uncertainty in nonlinear structural finite element model updating by numerical simulation of building structures. *Struct Control Health Monit*. 26(3): p.e2297.

Bernal D., Döhler M., Kojidi S.M., Kwan K., Liu Y. (2015). First mode damping ratios for buildings. *Earthquake Spectra*. 31(1):367–81

Eads L., Miranda E., Lignos D.G. (2015). Average spectral acceleration as an intensity measure for collapse risk assessment. *Earthq Eng Struct Dyn*. 44(12):2057–73

Elkady, A. (2016). Collapse risk assessment of steel moment resisting frames designed with deep wide-flange columns in seismic regions. Ph.D. thesis, McGill Univ., Montreal.

Elkady A., Lignos D.G. (2014). Modeling of the composite action in fully restrained beam-to-column connections. *EESD* 43(13):1935–54

FEMA (2009). Quantification of Seismic Performance Factors, FEMA P-695 Report, prepared by the Applied Technology Council for Federal Emergency Management Agency, Washington, DC

Gao Y., Mosalam K.M. (2018). Deep Transfer Learning for Image-Based Structural Damage Recognition. *Computer-Aided Civil and Infrastructure Engineering*. 33(9):748–68

Gokkaya B.U., Baker J.W., Deierlein G.G. (2016). Quantifying the impacts of modeling uncertainties on the seismic drift demands and collapse risk of buildings. *Earthq Eng Struct Dyn*. 45(10):1661–83

Huang H., Burton H. V. (2019). Classification of in-plane failure modes for reinforced concrete frames with infills using machine learning. *Journal of Building Engineering*. 25: p.100767.

Ibarra L., Krawinkler H. (2011). Variance of collapse capacity of SDOF systems under earthquake excitations. *Earthq Eng Struct Dyn*. 40(12):1299–1314

Ibarra L.F., Medina R.A., Krawinkler H. (2005). Hysteretic models that incorporate strength and stiffness deterioration. *Earthq Eng Struct Dyn*. 34(12):1489–1511

Karbassi A., Mohebi B., Rezaee S., Lestuzzi P. (2014). Damage prediction for regular reinforced concrete buildings using the decision tree algorithm. *Comput Struct*. 130:46–56

Kazantzi A.K., Vamvatsikos D., Lignos D.G. (2014). Seismic performance of a steel moment-resisting frame subject to strength and ductility uncertainty. *Eng Struct*. 78:69–77

Kiani J., Camp C., Pezeshk S. (2019). On the application of machine learning techniques to derive seismic fragility curves. *Comput Struct*. 218:108–22

Krawinkler H., F. Zareian, D.G. Lignos, L.F. Ibarra (2010) “Significance of Modeling Deterioration in Structural Components for Predicting the Collapse Potential of Structures under Earthquake Excitations.” In M. Fardis (Ed.), *Performance-Based Earthquake Engineering*. Ed. Springer.

Liel A.B., Haselton C.B., Deierlein G.G., Baker J.W. (2009). Incorporating modeling uncertainties in the assessment of seismic collapse risk of buildings. *Structural Safety*. 31(2):197–211

Lignos D.G., Hartloper A.R., Elkady A., Deierlein G.G., Hamburger R. (2019). Proposed Updates to the ASCE 41 Nonlinear Modeling Parameters for Wide-Flange Steel Columns in Support of Performance-Based Seismic Engineering. *Journal of Structural Engineering*. 145(9): p.04019083

Lignos D.G., Krawinkler H. (2011). Deterioration Modeling of Steel Components in Support of Collapse Prediction of Steel Mom. Frames under Earth. Loading. *Journal of Struct. Eng.* 137(11):1291–1302

Mahmoudi S.N., Chouinard L. (2016). Seismic fragility assessment of highway bridges using support vector machines. *Bulletin of Earthquake Engineering*. 14(6):1571–87

Mangalathu S., Heo G., Jeon J.S. (2018). Artificial neural network based multi-dimensional fragility development of skewed concrete bridge classes. *Eng Struct*. 162:166–76

Mangalathu S., Jeon J.S. (2018). Classification of failure mode and prediction of shear strength for reinforced concrete beam-column joints using machine learning techniques. *Eng Struct*. 160:85–94

Mazzoni S., Mckenna F., Scott M.H., Fenves G.L., Ili A. (2006). Open System for Earthquake Engineering Simulation (OpenSees) OpenSees Command Language Manual

McKenna F.T. (1997). *Object-Oriented Finite Element Programming: Frameworks for Analysis, Algorithms and Parallel Computing*. University of California, Berkeley.

Roeslin S., Ma Q., Juárez-Garcia H., Gómez-Bernal A., Wicker J, Wotherspoon L. (2020). A ML damage prediction model for the 2017 Puebla-Morelos, MX, earthquake. *Earth. Spectra*. 36(2):314–39

Sun, H., Burton, H. V., Huang, H. (2021). Machine learning applications for building structural design and performance assessment: State-of-the-art review. *Journal of Building Engineering*, 33, 101816.

Vamvatsikos D., Allin Cornell C. (2002). Incremental dynamic analysis. *EESD* 31(3):491–514

Zhang Y., Burton H. V., Sun H., Shokrabadi M. (2018). A machine learning framework for assessing post-earthquake structural safety. *Structural Safety*. 72:1–16